Demonstration of ocean surface salinity microwave measurements from space using AMSR-E data over the Amazon plume

N. Reul,[1] S. Saux-Picart,[1] B. Chapron,[1] D. Vandemark,[2] J. Tournadre,[1] and J. Salisbury[2]

[1] Microwave Sea Surface Salinity (SSS) measurements can be performed by isolating the emissivity response to salinity changes from numerous geophysical effects, including surface temperature and wind waves. At L-band frequencies (1 to 2 GHz), the sensitivity to SSS is sufficient but it falls off quickly as frequency is increased. Nevertheless, methods using higher microwave frequencies with much lower SSS sensitivity than at L band, can already be tested. In particular, combining 6 and 10 GHz data in vertical polarization efficiently minimizes sea surface roughness and thermal impacts. Using AMSR-E data, the retrieved bi-monthly maps of SSS at $0.5°$ resolution over the region of the Amazon plume show relative accuracy in-line with the future L-band dedicated mission objectives. **Citation:** Reul, N., S. Saux-Picart, B. Chapron, D. Vandemark, J. Tournadre, and J. Salisbury (2009), Demonstration of ocean surface salinity microwave measurements from space using AMSR-E data over the Amazon plume, *Geophys. Res. Lett.*, *36*, L13607, doi:10.1029/2009GL038860.

1. Introduction

[2] Ocean surface microwave emission is controlled by a variety of physical and chemical factors such as temperature and salinity as well as wave-generated surface roughness, foam and spray. The sensitivity of the emitted radiation to small variations in such factors is a function of frequency, probing angle and polarization state.

[3] Low frequency microwave radiometers onboard the ESA's Soil Moisture and Ocean Salinity (SMOS) and the NASA Aquarius missions have been selected and will soon provide the first global measurements of SSS dynamics from space, with an expected resolution of the order of 0.1 psu (practical salinity unit). SMOS and Aquarius sensors will operate at an L-band frequency of ~1.4 GHz, chosen as a trade-off between good sensitivity to SSS and reasonable spatial resolution. Yet, this study demonstrates that there already exists a capability in space to retrieve and refine ocean satellite salinity measurements and methods. We utilize the C- and X-band data from the Advanced Microwave Scanning Radiometer - Earth Observing System (AMSR-E). While these bands have significantly lower SSS sensitivity than that at L-band, they offer an opportunity to evaluate salinity inversion budget issues - this using on-orbit data with temporal and horizontal resolution scales in line with or exceeding the coming missions.

[4] To retrieve SSS from C (6.9 GHz) and X (10.7 GHz) - band T_Bs, there are a number of challenging issues that must be considered. At AMSR-E incidence angle near $55°$, the SSS sensitivity in vertical polarization (V-pol) is larger than that at horizontal polarization (H-pol), and the warmer the sea surface, the more sensitive is T_B to SSS (according to *Klein and Swift* [1977] (KS) dielectric constant model). The shift from L-band to C- and X-bands lowers T_B sensitivity to changes in salinity by a factor of 10 to 20. At an SST ~30°C and at an incidence angle of $55°$, the sensitivity reaches a V-pol maximum magnitude of about 0.06 K/psu, and 0.03 K/psu, at C- and X-bands, respectively, whilst at L-band, it is ~0.9 K/psu. Moreover, the T_B sensitivity to SST is $0.6-0.7$ K/°C at these frequencies, i.e. about ten times higher than the impact of a 1 psu change in SSS. Finally, surface waves can cause significant changes in the observed brightness temperature that may mask the weak salinity signature.

[5] Given this expected weak sensitivity, this study is limited to the Amazon plume region in the Northwestern Tropical Atlantic characterized by large ($100-200$ km) and persistent salinity contrasts that exceed the 0.1 psu salinity science mission requirement by a large factor of $10-100$, and by warm surface waters. This region is of great importance within the L-band salinity mission context due to the large freshwater flux from the discharge of the Amazon and Orinoco rivers, and their interactions with the North Brazil (NBC) and Guiana currents.

[6] To minimize the impact of competing terms carried in the ocean T_B measurements, we use a T_B difference quantity obtained with AMSR-E data, $\Delta T_B^v = T_v^{6.9} - T_v^{10.7}$, where $T_v^{6.9}$ and $T_v^{10.7}$ are the T_B at the ocean surface in V-pol at C- and X-band, respectively. This quantity is selected because (i) it strongly minimizes the SST impact while weakly affecting the sensitivity to SSS (according to KS's model, at SST = 30°C, $\partial \Delta T_B^v / \partial SSS \simeq -0.05$ K/psu and $\partial \Delta T_B^v / \partial SST \simeq 0.025$ K/°C), and (ii) $T_v^{6.9}$ and $T_v^{10.7}$ respond similarly to changes in surface wind speed from about 4 to 10 m.s^{-1}, hence ΔT_B^v exhibits on average very little sea surface roughness dependence.

[7] SSS is retrieved in the Northwestern Tropical Atlantic by minimizing the difference between AMSR-E satellite estimates of ΔT_B^v along swath and predictions from the KS's model. Bi-monthly and monthly average AMSR-E SSS retrievals for year 2003 are then compared with co-located *in situ* upper layer salinity measurements. In addition, to support spatial validation in this study, we used satellite-derived colored dissolved organic matter (CDOM) maps as a proxy for delineating the spatial extent and patterns of the Amazon and Orinoco freshwater plumes [e.g., *Hu et al.*, 2004].

2. Data

[8] The AMSR-E instrument onboard the NASA EOS Aqua satellite is a forward-looking, conically scanning radi-

[1]Laboratoire d'Océanographie Spatiale, Institut Francais de recherche et d'Exploitation de la Mer, Plouzané, France.
[2]Ocean Processes Analysis Laboratory, University of New Hampshire, Durham, New Hampshire, USA.

ometer operating at 55° incidence and 9 frequencies between 6.9 and 89 GHz. We use the 6.9 and 10.7 GHz L2A T_B product, resampled at 56 km spatial resolution, from the National Snow and Ice Data Center (NSIDC). The radiometer noise for 6.9 GHz and 10.7 GHz observations along scan is 0.3 K and 0.6 K, respectively. During the L2A processing, adjacent observations are averaged to reduce the noise to 0.1 K.

[9] In addition, we used the L2B ocean swath product [*Wentz and Meissner*, 2000], also available at NSIDC, that contains SST, near-surface wind speed, columnar water vapor, columnar cloud liquid water, and quality flags. The L2B ocean products, including SST, are retrieved by applying a climatological salinity correction to the L2A T_B data. Therefore, variation in actual SSS from climatology may have an impact on the retrieved AMSR-E SST, which in turn, may affect the quality of the SSS retrieval. To minimize this potential effect, we used the merged AMSR-AVHRR analysis product developed by *Reynolds et al.* [2007] as the ancillary SST. Available at the National Climatic Data Center (NCDC), these SST products have a spatial grid resolution of 0.25° and a temporal resolution of 1 day. Systematic biases (such as the SSS impact on AMSR-E SST) on this merged SST product is reduced because (i) it includes a large-scale adjustment of satellite biases with respect to in situ data and (ii) because the error characteristics of both infrared and microwave instruments are independent. Note as well that this product is based on night-time acquisitions to avoid diurnal cycle signatures.

[10] To demonstrate that AMSR-E retrieved SSS products contain enhanced information with respect to climatologies, we develop a match-up data set between AMSR-E bi-monthly averaged SSS estimates and in situ data provided at the French Coriolis Argo Data center. The in situ data originate from different sources such as profile data (selected at the uppermost level located between 5 m and 10 m depth), with the addition of underway collection on research vessels and voluntary observing ships (VOS), and from moorings in the tropical Atlantic (PIRATA array). The monthly SSS climatology of the tropical Atlantic developed by *Reverdin et al.* [2007] and generated at a spatial resolution of 1° × 1° is also used in the present work. The satellite-derived maps of CDOM absorption coefficient derived at 443 nanometers (a_{cdom}(443)), as a proxy to detect patches of low salinity surface waters, come from the monthly merged data product (9 km resolution) obtained through the NASA/Giovanni server (http://reason.gsfc.nasa.gov/OPS/Giovanni). It is a composite of SeaWiFS and MODIS products derived using the Garver-Siegel-Maritorena [*Maritorena et al.*, 2002] semi-analytical ocean optics model. This product provides a CDOM estimate similar to the absorption retrieval approach of *Hu et al.* [2004] and will be noted as a_{cdom} in the remainder of the paper. All datasets were compiled for the year 2003 over the spatial domain between 20° S and 20° N and 70° W and 20° W.

3. Methods

[11] AMSR-E Swath data flagged for rain, low sun glint angles and low Geostationary Radio Frequency Interference (RFI) angles were first discarded. The vertically polarized

L2A T_B products at each AMSR-E frequency f, hereafter denoted $\tilde{T}_v^f$, can be expressed as

$$\tilde{T}_v^f = T_{up}^f + \tau^f \left[e_v^f T_s + r_v^f (\tilde{\Omega}_v^f T_{down}^f + \tau^f T_C) \right] \quad (1)$$

where e_v^f is the sea surface emissivity in v-pol and the corresponding reflectivity is $r_v^f = 1 - e_v^f$. T_{up}^f is the upwelling atmospheric brightness temperature at the top of the atmosphere, T_{down}^f is the downwelling atmospheric brightness temperature at the surface, τ^f is the atmospheric transmissivity and T_s is the SST. $T_C \sim 2.7$ K is the cosmic background radiation temperature. The $\tilde{\Omega}_v^f$ term is a correction factor to account for nonspecular reflection of the atmospheric downwelling radiation from the rough surface. Given the AMSR-E Level2B water vapour, cloud liquid water and surface wind speed products, as well as the co-localized daily AVHRR-AMSR SST products, T_{up}^f, T_{down}^f, τ^f and $\tilde{\Omega}^f$ can be evaluated using the algorithm described by *Wentz and Meissner* [2000]. The surface reflectivity in v-pol at frequency f can then be estimated using equation (1) as:

$$r_v^f = \frac{\tilde{T}_v^f - T_{up}^f - \tau^f T_s}{\tau^f \left[\tilde{\Omega}_v^f T_{down}^f + \tau^f T_C - T_s \right]} \quad (2)$$

Using equation (2), the difference ΔT_b^v in brightness temperature estimated at the surface level between 6.9 GHz ($T_v^{6.9}$) and 10.7 GHz ($T_v^{10.7}$) vertical polarization channels is

$$\Delta T_b^v = T_v^{6.9} - T_v^{10.7} = T_s \left(r_v^{10.7} - r_v^{6.9} \right) \quad (3)$$

where ΔT_b^v includes the sum of two contributions. The first one is the difference in the flat surface ocean reflectivity between the two channels (Δr_{flat}) and the second is due to a possibly differing surface roughness impact on the reflectivity (Δr_{rough}) at the two frequencies [*Webster et al.*, 1976]. To evaluate the latter effect, the estimated surface quantity $r_v^{10.7} - r_v^{6.9}$ was averaged over ±1 m/s AMSR-E wind speed bins and ±1°C sea surface temperature bins. The results of the averaging done over all data for year 2003 are shown in Figure 1 together with the superimposed wind speed probability distribution function (blue curve). As illustrated, within the most populated wind speed conditions from about 4 to 10 m/s, $r_v^{10.7} - r_v^{6.9}$ is very weakly wind speed dependent at the different SST conditions encountered. At the rarely occurring low and high wind speed conditions, the reflectivities at each frequency are not evolving similarly as function of wind speed (likely due to differing surface waves and foam impact). Although the roughness impact can be significant in these rare conditions, we assume here that on average $\Delta r_{rough} \simeq 0$.

[12] Thus, the SSS retrieval methodology from the estimated ΔT_b^v follows. First, we evaluate Δr_{flat} using KS's model applied to the AVHRR-AMSR SST and for salinity values ranging from 0 to 40 psu. The retrieved SSS along swath is then determined by minimizing the difference between the KS prediction and the AMSR-E ΔT_b^vs. Swath retrieved SSS is then mapped onto a 0.5° resolution grid,
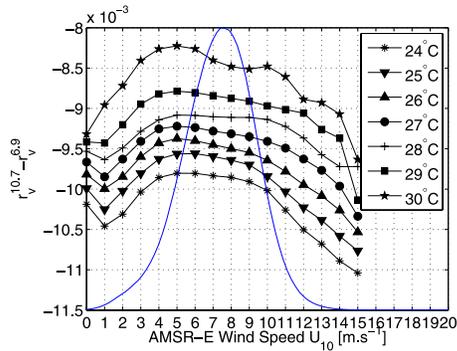
Figure 1. Difference in sea surface reflectivities between X and C bands averaged over ±1 m/s AMSR-E wind speed bins and ±1°C sea surface temperature bins (centered at the SST values given in the legend). The averaging is done over all data within the spatial domain between 20° S and 20° N and 70° W and 20° W, for year 2003. The blue curve indicates the probability density function of AMSR-E wind speed value (artificially normalized to match the y-axis scale). The values at 0 m/s are obtained from the Klein and Swift model evaluated at SSS = 36 psu.

averaged over 15 days or 1 month periods and spatially smoothed by a 1° by 1° moving average.

4. Results

[13] We illustrate the methodology by considering here the results for July 2003. The monthly-averaged ΔT_b^v and SST maps are shown in Figure 2. Between July and February, the

surface layer of the NBC separates from the coast at around 7°–8°N and retroflects with its waters feeding the North Equatorial Countercurrent, in a process known as North Brazil Current retroflection. Patches of high ΔT_b^v values exceeding their surrounding water counterparts by more than 0.4 K are observed centered near 7°N 50°W and following the NBC retroflection. As illustrated in Figure 2d, assuming a constant salinity of 36 psu along a north-west/south-east section across these patches, KS applied to the AMSR-AVHRR SST predicts that the evolution of ΔT_b^v along that section cannot be explained solely by the spatial changes in SST (red curve). The model prediction for ΔT_b^v, assuming that SSS along the transect evolves as in the monthly climatology (blue curve), shows a much better agreement with the data, although significant local differences can be observed around the measured ΔT_b^v peak. This analysis strongly suggests that the large amplitude ΔT_b^v variations observed within the domain (0°N–20°N, 70°W–40°W) are dominated by the impact of SSS variations.

[14] The July 2003 monthly composite map of the CDOM absorption coefficient (see Figure 3a) clearly shows that the area where ΔT_b^v exceed about −2.5 K systematically exhibit high a_{cdom} values. This further indicates the potential signature of the Amazon plume in AMSR-E signals. The monthly-averaged AMSR-E retrieved SSS map given in Figure 3b shows that these areas indeed correspond to predicted patches of low-salinity water (below 35–34 psu). The extent and dispersal patterns of the Amazon freshwater plume seen by AMSR-E is well correlated with the highly colored waters, as indicated by the superimposed a_{cdom} contours on the SSS map of Figure 3.

[15] In July 2003, the voluntary observing ships (VOS) MN/Colibri, equipped with a thermo-salinograph, performed
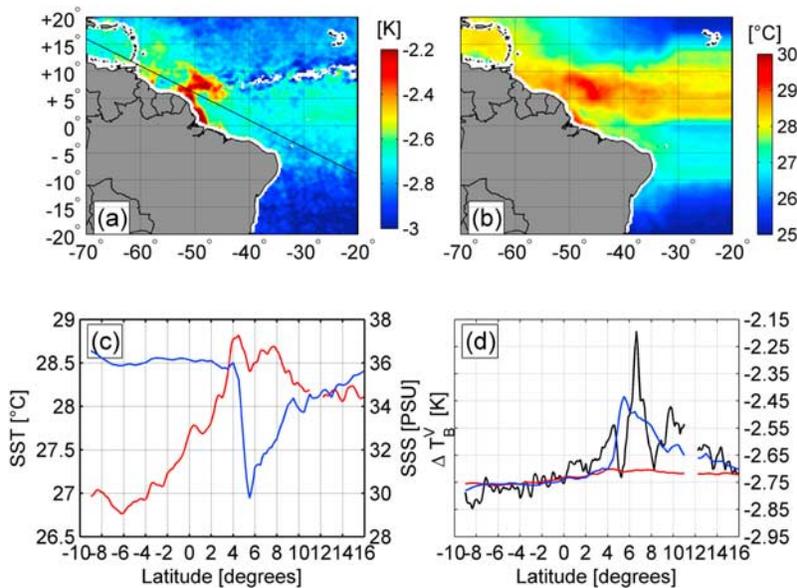

Figure 2. (a) Monthly averaged difference $<\Delta T_b^V>$ in estimated flat sea surface brightness temperature between 6.9 and 10.7 GHz frequencies in vertical polarization, and for the month of July 2003. The black line illustrates the location of the transect shown in Figures 2c and 2d. (b) Corresponding monthly averaged AVHRR-AMSR OI 0.25° sea surface temperatures. (c) Sea surface temperature from AVHRR-AMSR (red curve) and salinity from the monthly climatology of the tropical Atlantic (blue curve) along the transect shown in Figure 2a. (d) Corresponding $<\Delta T_b^V>$ along the transect measured from AMSR-E (black) and estimated using Klein and Swift's dielectric constant model applied to AVHRR-AMSR SST and (i) to a constant salinity of 36 psu (red) or (ii) to the surface salinity from the climatology (blue).
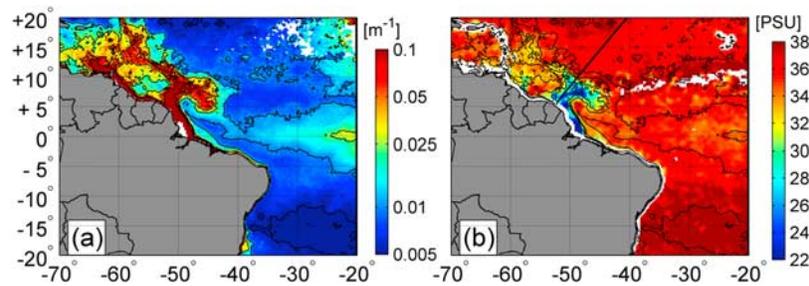
Figure 3. (a) Monthly composite map of a_{cdom} obtained with the GSM model and the SeaWiFS and MODIS sensors for July 2003. (b) Monthly averaged sea surface salinity retrieved from AMSR-E. The thick black line shows the July 2003 transect of the ship MN/Colibri, equipped with an underway thermosalinograph. Thin black curves in both figures represent contours of a_{cdom} at 0.005, 0.01, 0.025, 0.05 and 0.1 m^{-1}.

SSS measurements along the transect shown in Figure 3b, collecting seawater at about 5 m depth. The SSS measured by the ship is shown in Figure 4a, together with the 15 day-average retrieved AMSR-E SSS and the July climatology interpolated along the transect. The large-scale spatial structure of the freshwater Amazon plume, extending about 600 km offshore, is clearly observed in the AMSR-E SSS product. On the other hand, the climatology strongly underestimates the salinity gradient across the plume. Local discrepancies between the satellite and in situ SSS are nevertheless observed at scales smaller than about 100 km. Comparison results similar to this July example are found throughout the year, and the satellite SSS data capture the seasonal cycle in the extent and dispersal patterns of the Amazon and Orinoco plumes. Regardless of the season, note that the measured ΔT_B are corrected for a constant bias of ~-0.15 K to align the mean satellite-retrieved SSS to the in situ and climatological values. It may indicate an absolute calibration offset between the two AMSR-E frequency channels in 2003.

[16] The overall in situ - satellite data collocation are shown in Figure 4b. The root-mean square (rms) difference between all in situ and satellite observations is 1.5 psu. The rms within ±2-psu bins extending from 19 to 39 psu was also evaluated: it decreases from about $3-5$ psu at the lowest SSS down to about 1 psu, achieved for salinities higher than about 35 psu. The strong spatio-temporal variability of the plume may contribute to generate significant differences when comparing in situ measurements with large footprint satellite products sampled at a 0.5° resolution and averaged over 15 days. Another source is possibly be the differing salt content in the vertical as probed by very near surface satellite measurements (sub cm) and deeper-level in situ observations, usually conducted at depth between 5 to 10 m. Moreover, errors in the retrieval algorithm are certainly included due to (i) neglecting the difference in the roughness impact between the two channels at low and high winds (ii) errors in the ancillary geophysical products, such as SST (e.g., not accounting for a diurnal SST cycle of 1°C amplitude at a mean SST of ~27°C shall induce SSS retrieval errors ranging from ~0.5 to 2 psu, according to KS's model) (iii) errors in the atmospheric contribution removal, (iv) residual model error in the dielectric constant (KS model claims a residual model error in brightness temperature of 0.09K, which is the

noise level of the averaged AMSR data), and (v) instrumental noises. Similar factors and data intercomparison issues will also be present in the coming L-band mission calibration and validation activities. The encouraging point is that this study demonstrates that, even using sensors at least 10 times less sensitive to SSS than the future L-band missions, monthly and bi-monthly surface salinity can be retrieved with a relative accuracy that is in line with the future dedicated mission objectives. The method we developed can be readily applied in tropical oceans region with the largest river plumes both to derive new satellite-based SSS climatologies of the plumes as well as to characterize the seasonal cycles and interannual variability of their associated large-scale surface salinity structures. And while AMSR-E can be used to begin the new era of global monitoring of surface salinity over the oceans, it may also prove useful to incorporate its independent estimates into the coming L-band SMOS and Aquarius SSS retrieval algorithms in the tropics.
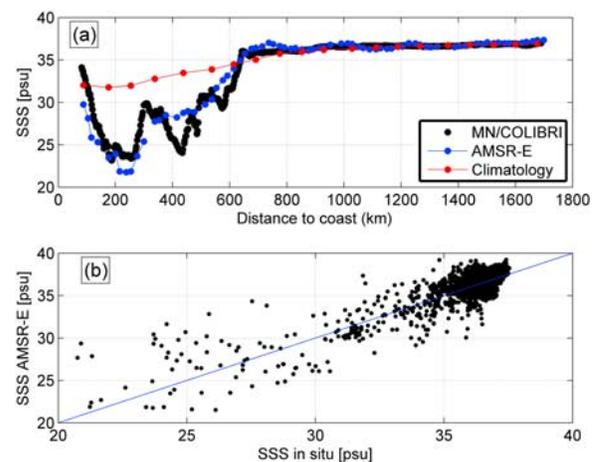

Figure 4. (a) Sea surface salinity measured by the MN/Colibri TSG (black dots), 15-days averaged retrievals from AMSR-E ΔT_b^V (blue dots) and July climatology (red dots) interpolated along the ship transect. (b) Comparison between co-localized AMSR-E SSS retrievals and in situ measurements over the year 2003. Root mean square difference is about 1.5 psu.

References

Hu, C., E. Montgomery, R. Schmitt, and F. Muller-Karger (2004), The dispersal of the Amazon and Orinoco River water in the tropical Atlantic and Caribbean Sea: Observation from space and S-Palace floats, *Deep Sea Res.*, *51*(10–11), 1151–1171.

Klein, L. A., and C. T. Swift (1977), An improved model of the dielectric constant of sea water at microwave frequencies, *IEEE Trans. Antennas Propag.*, *25*, 104–111.

Maritorena, S., D. A. Siegel, and A. Peterson (2002), Optimization of a semi-analytical ocean color model for global scale applications, *Appl. Opt.*, *41*(15), 705–2714.

Reverdin, G., E. Kestenare, C. Frankignoul, and T. Delcroix (2007), Surface salinity in the Atlantic Ocean (30°S–50°N), *Prog. Oceanogr.*, *73*(3–4), 311–340.

Reynolds, R. W., T. M. Smith, C. Liu, D. B. Chelton, K. S. Casey, and M. G. Schlax (2007), Daily high-resolution-blended analyses for sea surface temperature, *J. Clim.*, *20*(22), 5473–5496, doi:10.1175/2007JCLI1824.1.

Webster, W. J., T. T. Wilheit, D. B. Ross, and P. Gloersen (1976), Spectral characteristics of the microwave emission from a wind-driven foam-covered sea, *J. Geophys. Res.*, *18*, 3095–3099.

Wentz, F. J., and T. Meissner (2000), AMSR ocean algorithm, version 2, algorithm theoretical basis document, *RSS Tech. Rep. 121599A-1*, Remote Sens. Syst., Santa Rosa, Calif.

————————————
B. Chapron, N. Reul, S. Saux-Picart, and J. Tournadre, Laboratoire d'Océanographie Spatiale, Institut Français de recherche et d'Exploitation de la Mer, BP 70, F-29820 Plouzané CEDEX, France. (nreul@ifremer.fr)

J. Salisbury and D. Vandemark, Ocean Processes Analysis Laboratory, University of New Hampshire, Durham, NH 03824, USA.